Observation of Discrete Quadratic Solitons

R. Iwanow,[1] R. Schiek,[1] G. I. Stegeman,[1] T. Pertsch,[2] F. Lederer,[2] Y. Min,[3] and W. Sohler[3]

[1]Center for Research and Education in Optics and Lasers–School of Optics, University of Central Florida, 4000 Central Florida Boulevard, Orlando, Florida 32816-2700, USA
[2]Institute of Condensed Matter Theory and Solid State Optics, Friedrich-Schiller-Universität Jena, Max-Wien-Platz 1, D-07743 Jena, Germany
[3]Institute of Applied Physics, Universität Paderborn, D-33095 Paderborn, Germany

Discrete solitons with two frequency components mutually locked by a quadratic nonlinearity have been observed for the first time. Optical experiments have been performed in arrays of coupled channel waveguides with tunable cascaded quadratic nonlinearity. The tunability was the prerequisite that soliton species with different topology could be identified in the same array. Moreover, soliton stability has been experimentally probed. Good agreement with theoretical predictions was found.

Within the last decade nonlinear localization phenomena in lattices have attracted a steadily growing interest, and their existence has been predicted in a wide range of physical settings. The diversity of these phenomena and their richness compared to those in continuous systems stems essentially from the mutual interplay of the peculiar transport properties (diffusion, diffraction, dispersion, tunneling) with the specific nonlinearity of the lattice. In particular, the differences to continuous systems are significant if the lattice topology is such that the excitation dynamics may be described by the linear interaction of many nonlinear, but fairly simple unit cells. In this particular case the lattice is frequently termed a discrete system. Consequently, the respective localized structures are called discrete breathers or discrete solitons. Their wave vectors are situated in the semi-infinite gaps surrounding the eigenvalue bands of linear solutions. It is now well understood that solitons in various discrete systems (excitations in molecular chains [1], in Bose-Einstein condensates [2], light in waveguide arrays [3], etc.) share common features. Thus it is appropriate to experimentally study them in an accessible physical environment. Optical settings such as one- and two-dimensional arrays of coupled channel waveguides meet the requirements of easy handling, excitation, and visualization (see for an overview Ref. [4] and references therein). To date the experimental studies are restricted to frequency degenerate effects in media with Kerr, photorefractive, and orientational nonlinearities where various discrete solitons associated with diverse linear diffraction properties have been observed [5–8]. But because the very interplay between these linear transport phenomena and the nonlinearity governs the localization process, it is challenging to study localization phenomena for other more diverse nonlinearities. In this respect quadratic nonlinearities deserve particular attention because the interaction process involves two or three components at different frequencies and new degrees of freedom enter the dynamical process.

Different kinds of quadratic discrete solitons have been theoretically predicted to exist [9,10]. Just as for other nonlinearities it is convenient to study them in an optical environment, e.g., in an array of coupled single mode channel waveguides in a crystal with a strong second-order nonlinearity. Their continuous counterparts, i.e., multicolored or quadratic spatial solitons, have already been experimentally verified. It was shown that the wave-vector mismatch $\Delta\beta = 2\beta(\omega) - \beta(2\omega)$ between the participating waves is a crucial parameter, which determines the features of the respective soliton family [11]. The size and the sign of this mismatch govern the character of nonlinear phase modulation [12] which, together with the linear diffraction properties, controls the localization process.

In the array light is guided by the individual channels and spreads laterally by evanescent field coupling between adjacent channels. This gives rise to so-called "discrete diffraction" whose properties are radically different from diffraction in continuous media. Because of the periodic cosinelike shape of the diffraction relation, i.e., the variation of the longitudinal wave-vector component with the transverse one, diffraction can be managed ranging from normal, to zero, to anomalous diffraction [13,14]. Resting linear solutions with all waveguides excited in phase (unstaggered excitation) appear in the center of the Brillouin zone. Similar to continuous media, they experience normal diffraction. Resting antiphase solutions (staggered excitation) exist at the edges of the Brillouin zone, where diffraction is anomalous. This diffraction management can be easily achieved by varying the phase difference between modes in adjacent waveguides with a slight inclination of the input beam of a few degrees. To avoid coupling to linear waves, soliton solutions exist only with wave vectors outside the linear eigenvalue band and require thus positive (negative) nonlinear phase

modulation in the center (at the edges) of the Brillouin zone.

Here we report the first observation of these different kinds of discrete quadratic solitons. We prove that soliton topology changes if the nonlinear phase modulation changes sign achieved by changing the sign of the wave-vector mismatch. We observe in-phase (or unstaggered) solitons for $\Delta\beta > 0$, whereas they appear as out-of-phase (or staggered) species for $\Delta\beta < 0$. If the combination of phase modulation and diffraction is inappropriate for soliton formation, for example, in-phase excitation and $\Delta\beta < 0$, nonlinearly reinforced delocalization was observed as well [15].

The different soliton types can be further classified by their symmetry. "Even" solitons have the same power in two adjacent waveguides in the soliton center such that the maximum power is centered virtually between two guides. In contrast the maximum power of "odd" solitons is centered at a guide [9,10]. While odd solitons are theoretically predicted to be stable, their even counterparts are predicted to be unstable. These stability properties have also been verified in our experiments. In general, all experimental observations were in good agreement with the theoretical predictions.

Four waveguide arrays, each consisting of 101 coupled channel waveguides with propagation along the X axis, were fabricated on a $L = 7$ cm long Z-cut lithium niobate crystal by titanium in diffusion. TM_{00}-mode waveguide losses were 0.2 dB/cm for the fundamental wave (FW) at $\lambda \approx 1550$ nm and 0.4 dB/cm for its second harmonic (SH). Center-to-center channel separations of $d = 16$, 15, 14.5, and 14 μm resulted in different coupling strengths and thus interchannel half-beat coupling lengths $L_c = 25.5$, 15.74, 12.16, and 9.53 mm, respectively, for the FW TM_{00} mode, determined from the output intensity distribution for a single waveguide excitation [14]. A peculiarity of our array is that because of the stronger SH confinement the evanescent coupling between SH TM_{00} modes vanishes. The observed excellent linear diffraction patterns of the FW indicated almost ideal arrays with both uniform channels and channel spacing. The sample was periodically poled with a period of 16.75 μm by electric field poling to achieve phase matching between the TM_{00} modes for SH generation at elevated temperatures in the range of 220 °C. The required wave-vector mismatch can be adjusted by varying the sample temperature T. In our experiments the relation between the phase mismatch $\Delta\beta L$ and sample temperature T was measured to be $\Delta\beta L = 8.1(234 - T[°C])$.

For the experimental investigation of quadratic discrete solitons we used a fiber laser producing a 5-MHz train of bandwidth limited 9-ps-long pulses at a wavelength of 1557.3 nm. The pulses were stretched in a chirped fiber grating, amplified in a large area core fiber amplifier, and then recompressed in a bulk grating compressor to give

4 kW of peak power in nearly transform limited pulses 7.5 ps long. The recompressed pulses were spatially reshaped into elliptical beams 28 to 62 μm wide (full width at half maximum) and 3.5 μm high and focused onto the polished front facet of the waveguide array. With this setup we could launch the FW into the TM_{00} modes of the array waveguides with an overlap of 50% to 60%. We excited different arrays with Gaussian shaped FW input beams of different widths resembling closely the shape of the solitons. The SH was not seeded, and we relied on the generation of the appropriate SH soliton component during the propagation in the array. To reduce the average power in the waveguides we used a 1:10 chopper. The sample was heated in an oven both to minimize photorefractive effects and to adjust the wave-vector mismatch with temperature T. The output of the array was observed with separate cameras for the FW and the SH, and quantified by measuring temporally averaged output intensities and total powers.

Theoretical simulations provide insight into the soliton's propagation behavior. With our short pulse excitation, the spatiotemporal evolution of the mode amplitudes u_n (FW) and ν_n (SH) may be described by the well-established time-dependent coupled mode equations [16]

$$i\frac{\partial u_n}{\partial z} + i\delta\frac{\partial u_n}{\partial t} + c(u_{n+1} + u_{n-1}) + 2\gamma u_n^* \nu_n = 0,$$
$$i\frac{\partial \nu_n}{\partial z} + \Delta\beta\nu_n + \gamma u_n^2 = 0, \tag{1}$$

where c, δ, and γ are the linear coupling constant ($L_c = \pi/2c$), the group velocity mismatch, and the effective quadratic nonlinear coefficient, respectively. For our pulse lengths, the group velocity dispersion can be neglected. Discrete solitons are stationary solutions of
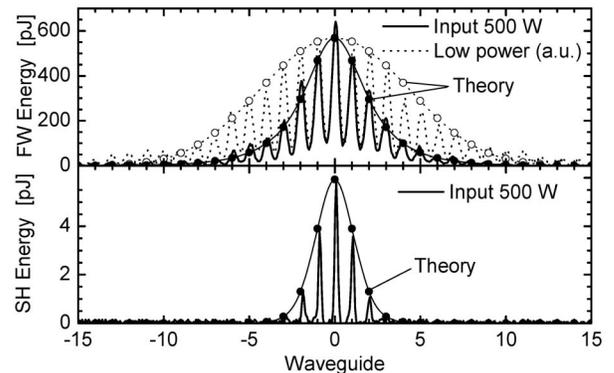

FIG. 1. Spatial pulse energy profile of the two nonlinearly coupled frequency components of an unstaggered odd discrete soliton ($\Delta\beta L = 140\pi$, $L_c = 15.7$ mm, FW input peak power of 500 W). Dotted lines and open circles show the low-power FW diffracted beam, and solid lines and circles show the soliton. Circles identify theoretical data.
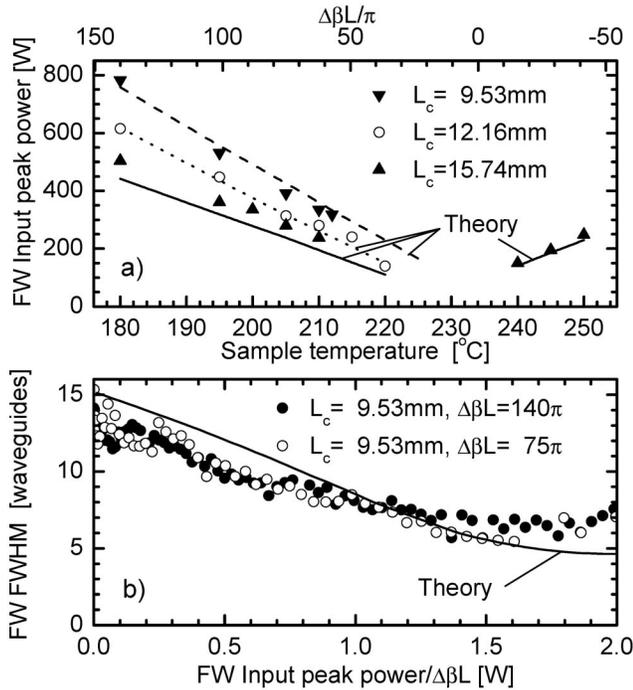
FIG. 2. (a) Soliton peak power versus $\Delta\beta L$ for arrays with different coupling lengths L_c. (b) FW output beam width versus the ratio FW input peak power/$\Delta\beta L$ for different $\Delta\beta L$.
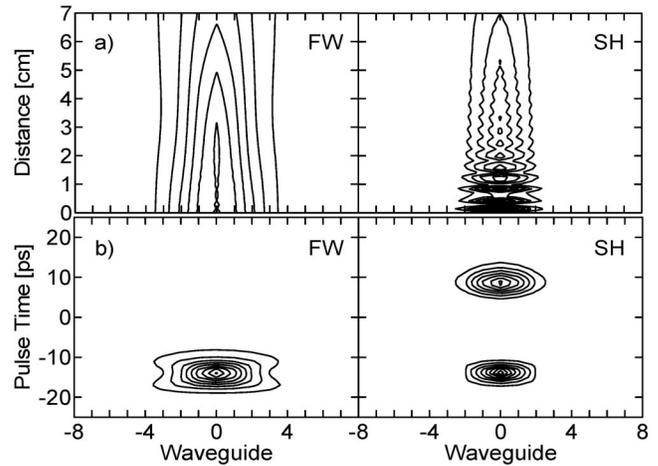

FIG. 3. (a) Simulated evolution of the transverse energy (time integrated) spatial profile of beams excited by a FW input ($\Delta\beta L = 140\pi$, $L_c = 15.7$ mm, FW input peak power of 442 W). (b) Spatiotemporal output distribution of the simulation in (a).

Eq. (1) [9,10]. The experimental findings were double-checked by solving this full set of Eqs. (1).

We started our experiments with the combination of positive $\Delta\beta L$ and normal diffraction, i.e., expecting to observe unstaggered solitons. Hence we focused the FW input beam untilted onto the sample, i.e., with a phase front parallel to the input facet, and the beam maximum centered at a waveguide. We increased the input power and observed a narrowing of FW and SH output beams until the width of the FW output equaled the width of the input beam. Figure 1 shows typical measured and simulated output intensity profiles for both wavelength components for an odd unstaggered soliton. The low-power FW diffraction pattern is also shown for comparison.

In order to obtain a more complete insight into the physics of soliton formation the experiments were repeated for several positive values of $\Delta\beta L$ (and thus positive nonlinear phase shift) and in different arrays with varying coupling. As expected from theoretical predictions, Fig. 2(a) (left side) confirms that the powers needed for soliton formation increased with the coupling strength and $\Delta\beta L$. The latter result is a clear indication of the quadratic nature of the nonlinear process, i.e., nonlinear phase modulation decreases with increasing $\Delta\beta L$. In Fig. 2(b) the measured beam width as a function of input power divided by $\Delta\beta L$ is plotted. It reproduces the theory well up to power levels equal to the soliton power. However, for powers well beyond the soliton power we observed delocalization and patterning effects not repro-

duced by our theoretical model. They might be due to remaining photorefraction, nonlinear induced absorption, and longitudinal sample inhomogeneities. These effects are expected to come into play for very high input powers and are not included in our theoretical modeling.

In Fig. 3(a) the evolution of the FW and the SH energy distribution of one pulse clearly indicates soliton behavior since the energy profile does not change significantly during the propagation. Moreover, the generation of the SH part of the soliton shortly after the input can be observed. The waveguide losses, although very small, are responsible for the power loss during the propagation. Furthermore, the simulations help to interpret the mea-
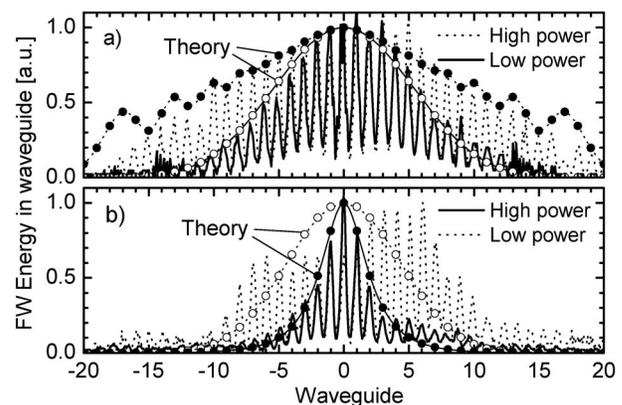

FIG. 4. (a) Nonlinear reinforced beam broadening for in-phase excitation ($\Delta\beta L = -50\pi$, $L_c = 12.16$ mm, FW input peak power of 1.4 kW). (b) Staggered soliton profile ($\Delta\beta L = -16\pi$, $L_c = 15.7$ mm, input peak power of 150 W). Solid and empty circles identify the high- and low-power theoretical data, respectively.
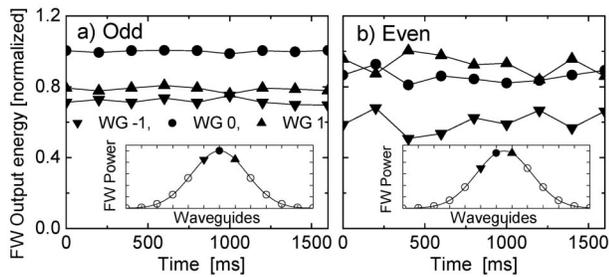
FIG. 5. Time sequence of FW output energies, sampled at intervals of 200 ms, from waveguides in the soliton center ($L_c = 15.7$ mm, $\Delta\beta L = 140\pi$). (a) Stable output for odd soliton excitation. (b) Unstable output for even excitation.

sured temporally averaged SH profiles, which in principle developed a complex temporal structure due to walk-off effects caused by unequal FW and SH group velocities. In general, most of the SH temporally overlaps the FW and represents the soliton's SH component. A second SH (radiation) pulse trails the soliton by the 24 ps walk-off time in a 7-cm-long sample. However, the calculated spatiotemporal distribution at the output, shown in Fig. 3(b), indicates soliton propagation for the mutually locked FW and SH. The spatial narrowing of the FW in the pulse center is evident. Although the soliton's SH component increases closer to phase matching, the SH radiation that has temporally walked away from the soliton increases even faster. Therefore an increasing part of the measured, temporally averaged, SH output no longer belongs to the soliton and a reliable SH soliton profile measurement is not clear for $|\Delta\beta L| < 20\pi$ with 7.5-ps-long pulses in our sample.

Next we investigated the beam evolution for a negative wave-vector mismatch and in-phase (unstaggered) as well as antiphase (staggered) excitation. The results are displayed in Fig. 4. As theory predicts, for unstaggered excitation we observed delocalization reinforced by nonlinearity [see Fig. 4(a)] because negative phase modulation reinforces normal diffraction. Bright soliton formation can be expected only for a staggered excitation at the edges of the Brillouin zone where diffraction is anomalous. The excitation with the required phase difference of π between modes in adjacent waveguides was realized by appropriately tilting the input beam by ~ 3 degrees. We observed the formation of odd staggered solitons with a typical FW profile shown in Fig. 4(b). The displayed nonideal low-power linear diffraction pattern is caused by our simple antiphase excitation setup with a tilted beam and the corresponding aberrations. The power for staggered soliton formation versus phase mismatch is shown on the right-hand side of Fig. 2(a).

Finally, the stability of the excited discrete solitons has been probed. Theory predicts that staggered as well as unstaggered odd solitons are stable, whereas the even ones are unstable. In agreement with this prediction we

found that very careful transverse beam alignment, with the input beam maximum centered on a channel, was necessary to obtain stationary output pictures of the soliton profiles. For example, different time frames in Fig. 5(a), taken at intervals of 200 ms, show stable powers in the three central waveguides of an odd unstaggered soliton ($\Delta\beta > 0$). When the input maximum was centered between two waveguides, a strongly flickering output as documented in the time frames of Fig. 5(b) was observed. The output profile's maximum jumped between the two waveguides adjacent to the input beam's maximum; i.e., the excitation tried to evolve into either of the two neighboring odd solitons. The observed instability was presumably seeded by small fluctuations in the pointing direction of the input beam due to vibrations in the optical mounts, etc. For staggered solitons ($\Delta\beta < 0$) a similar stability behavior has been observed.

In summary, we have presented the first experimental proof of both staggered and unstaggered stable discrete quadratic soliton propagation. Both soliton types have been excited in the same sample by merely changing the excitation conditions as beam tilt and wave-vector mismatch. Increased beam broadening was also measured for both the staggered and unstaggered excitations when the mismatch and thus the sign of phase modulation were chosen to reinforce instead of to cancel discrete diffraction.

———

[1] A. S. Davydov, J. Theor. Biol. **38**, 559 (1973).
[2] A. Trombettoni and A. Smerzi, Phys. Rev. Lett. **86**, 2353 (2001).
[3] D. N. Christodoulides and R. I. Joseph, Opt. Lett. **13**, 794 (1988).
[4] D. N. Christodoulides, F. Lederer, and Y. Silberberg, Nature (London) **424**, 817 (2003).
[5] H. S. Eisenberg et al., Phys. Rev. Lett. **81**, 3383 (1998).
[6] J. W. Fleischer et al., Nature (London) **422**, 147 (2003).
[7] D. Neshev et al., Opt. Lett. **28**, 710 (2003).
[8] A. Fratalocchi et al., Opt. Lett. **29**, 1530 (2004).
[9] T. Peschel, U. Peschel, and F. Lederer, Phys. Rev. E **57**, 1127 (1998).
[10] S. Darmanyan, A. Kobyakov, and F. Lederer, Phys. Rev. E **57**, 2344 (1998).
[11] R. Schiek et al., Opt. Lett. **29**, 596 (2004).
[12] G. I. Stegeman et al., Opt. Lett. **18**, 13 (1993).
[13] H. S. Eisenberg et al., Phys. Rev. Lett. **85**, 1863 (2000).
[14] T. Pertsch et al., Phys. Rev. Lett. **88**, 093901 (2002).
[15] R. Morandotti et al., Phys. Rev. Lett. **86**, 3296 (2001).
[16] T. Pertsch, U. Peschel, and F. Lederer, Opt. Lett. **28**, 102 (2003).